JOURNAL OF GEOPHYSICAL RESEARCH, VOL. 107, NO. D1, 4001, 10.1029/2001JD900253, 2002

Modeling interannual variability of water isotopes in Greenland and Antarctica

Martin Werner[1]
Max-Planck-Institute for Meteorology, Hamburg, Germany

Martin Heimann
Max-Planck-Institute for Biogeochemistry, Jena, Germany

Received 18 September 2000; revised 20 July 2001; accepted 26 July 2001; published 1 January 2002.

[1] A simulation with the Hamburg atmospheric general circulation model ECHAM-4, forced with sea surface temperatures of the period 1950–1994 and with stable water isotopes $H_2{}^{18}O$ and HDO explicitly included in the water cycle, was performed to examine interannual to decadal variations of the isotopic composition of precipitation in Greenland and Antarctica. The analyses focus on the Summit region, central Greenland, and the Law Dome region, East Antarctica, respectively. Simulation results reveal that about one third of the simulated variability in $H_2{}^{18}O$ can be explained by simultaneous changes of the surface temperature at the precipitation sites. Other climate variables influencing the isotope signal are identified by multiple linear regression, and the results show that the $H_2{}^{18}O$ record in central Greenland integrates the climatic history of a broader region. For the Law Dome region in Antarctica the $H_2{}^{18}O$ record appears to be mainly related to climate changes at the precipitation site only. For the deuterium excess a clear influence of climate condition at two distinct regions of the Indian Ocean on the simulated deuterium excess record of the Law Dome region is found. On the contrary, a reconstruction of the year-to-year variability of the deuterium excess signal in central Greenland, by Atlantic Ocean surface parameters only, fails. Additional correlation analyses between the ECHAM-4 isotope simulation and indices of the North Atlantic Oscillation (NAO) and the El Niño-Southern Oscillation phenomenon (ENSO) enable the detection of influenced regions in Greenland and Antarctica: While NAO and ENSO are imprinted in the simulated $H_2{}^{18}O$ record of precipitation, they cannot be detected in the simulated deuterium excess record. *INDEX TERMS:* 1827 Hydrology: Glaciology (1863); 3319 Meteorology and Atmospheric Dynamics: General circulation; 3344 Meteorology and Atmospheric Dynamics: Paleoclimatology; 3349 Meteorology and Atmospheric Dynamics: Polar meteorology; *KEYWORDS:* Water isotopes, general-circulation model, ice core records, interannual changes, Greenland, Antarctica

1. Introduction

[2] For more than 3 decades, measurements of stable water isotopes $H_2{}^{18}O$ and HDO have been used as proxy data for surface temperatures in paleoclimatological studies. Strong spatial correlations between the isotopic composition of precipitation (in general, expressed as the deviation from a standard water isotope sample, e.g., for $H_2{}^{18}O$:$\delta^{18}O = [(^{18}O/^{16}O)_{Sample} / (^{18}O / ^{16}O)_{V\text{-}SMOW}] - 1$, with V-SMOW = Vienna standard mean ocean water, and accordingly for $HD^{16}O$ and δD) and surface temperatures were first described by *Dansgaard* [1964]. Since then, past temporal changes of $\delta^{18}O$, e.g., measured in ice cores, are interpreted as changes of temperatures at the precipitation site. Within the ice core archive, the isotope records of Greenland and Antarctica are of special interest. Because of their remote geographical position and the rather stable polar climate, the isotope-temperature-relation is assumed to be well preserved there. However, for different climatic stages, such as the Younger Dryas period or the Last Glacial Maximum (LGM), new isotope-independent temperature estimates from both Greenland and Antarctica [*Jouzel*, 1999, and references therein] challenge the (spatial) calibration of the isotope thermometer, but not the close temporal relation between the isotopic signal and surface temperatures in general. On a much shorter monthly to seasonal timescale, a close temporal relation between the isotopic composition of precipitation and surface temperatures has also been observed for both polar regions [e.g., *Shuman et al.*, 1995; *van Ommen and Morgan*, 1996]. However, little is known about the cause of the year-to-year variability of $\delta^{18}O$ and δD in precipitation for the present climate. So far, any attempt to interpret the observed variability of $\delta^{18}O$ and δD measured in ice cores from both Greenland and Antarctica has been difficult because of the lack of long-term in situ observational climate records possibly related to the isotope signal, e.g., the temperature at the precipitation site [e.g., *White et al.*, 1997]. In addition, postdepositional effects (wind drift, relayering of snow, diffusion of the isotope signal) might add some noise to the δ values in the firn and hence complicate the interpretation of the observed isotope variability in polar snow. Nevertheless, in the recent past some attempts have been made to correlate either the isotopic signature of precipitation or interannual changes of the precipitation amount itself with large-scale circulation pattern changes such as the North Atlantic Oscillation (NAO) [*Appenzeller et al.*, 1998] or the El Niño-Southern Oscillation phenomenon (ENSO) [*Bromwich et al.*, 2000].

[3] In this study, we will apply a different approach by using an atmospheric general circulation model (AGCM) with both water

[1]Now at Max-Planck-Institute for Biogeochemistry, Jena, Germany.

0148-0227/02/2001JD900253$09.00

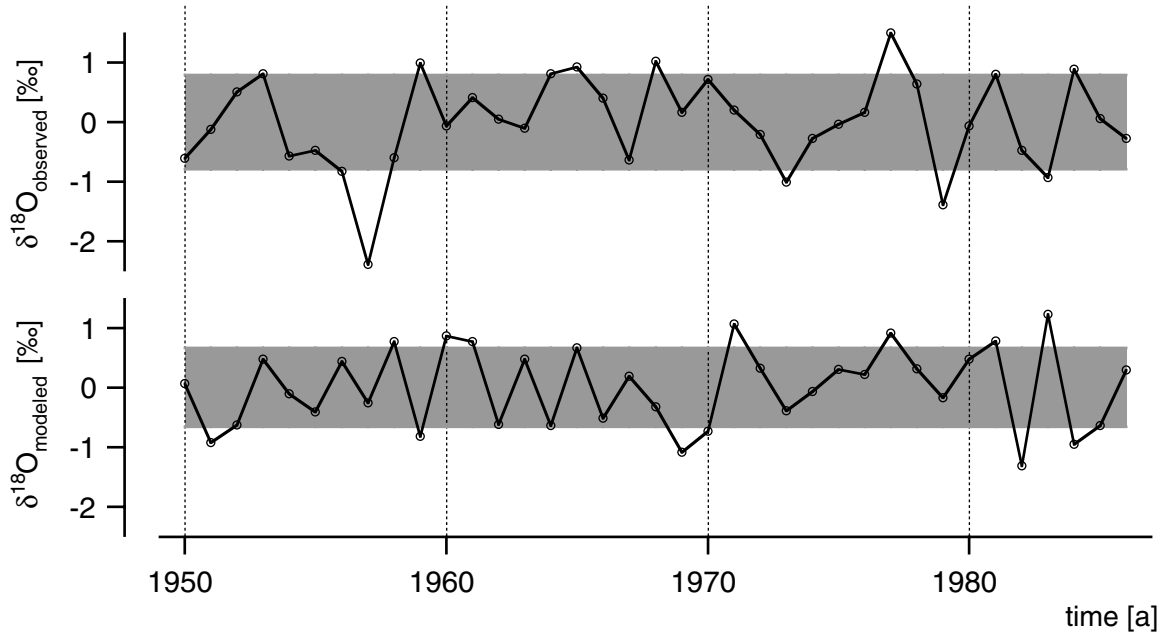

Figure 1. Comparison of (top) the observed stacked annual GRIP/GISP2 isotope anomalies (data compiled from *White et al.* [1997]) and (bottom) the modeled annual ECHAM-4 isotope anomalies of the grid box enclosing Summit, Greenland. The shaded area represents the calculated 1σ standard deviation of each time series.

isotopes $H_2{}^{18}O$ and HDO explicitly built into the hydrological cycle of the model. Isotope modeling with AGCMs has been shown to be a helpful tool to study the important mechanisms influencing the δ signals of precipitation for various climatic boundary conditions [e.g., *Charles et al.*, 1994; *Hoffmann et al.*, 1998; *Joussaume et al.*, 1984; *Jouzel et al.*, 1987]. In contrast to field measurements, all climate variables of an AGCM simulation which affect the isotopic fractionation processes are known. This enables a rigorous test of potential variables influencing the isotope signal to determine the variables most strongly related to the isotope anomalies. For example, *Cole et al.* [1999] reported a weak correlation between isotopes in precipitation and temperatures for only certain continental regions, mostly of the extratropics, in a 12-year AGCM simulation.

[4] Modeling of both $H_2{}^{18}O$ and HDO allows an additional analysis of the deuterium excess d (defined as $d = \delta D - 8\delta^{18}O$). Changes of the deuterium excess signal are mainly controlled by kinetic fractionation effects during evaporation and can therefore be used as an indicator of changes in temperature and humidity at the evaporation site [*Johnsen et al.*, 1989; *Merlivat and Jouzel*, 1979; *Vimeux et al.*, 1999]. Thus the strength of the correlation between climate conditions at potential evaporation sites and simultaneous changes of the deuterium excess signal in polar regions on an interannual timescale can also be tested by the described AGCM approach.

[5] Here we present results of an AGCM isotope experiment covering the period 1950–1994, and our analyses focus on the following questions: (1) Is the isotopic composition of precipitation of Greenland and Antarctica a reliable proxy for surface temperatures on interannual to decadal timescales? (2) Which other climate variables are of importance to explain the simulated variability in the $\delta^{18}O$ signal? (3) Is it possible to identify certain evaporation regions which mainly affect the simulated interannual variability of the deuterium excess over Greenland and Antarctica, respectively?

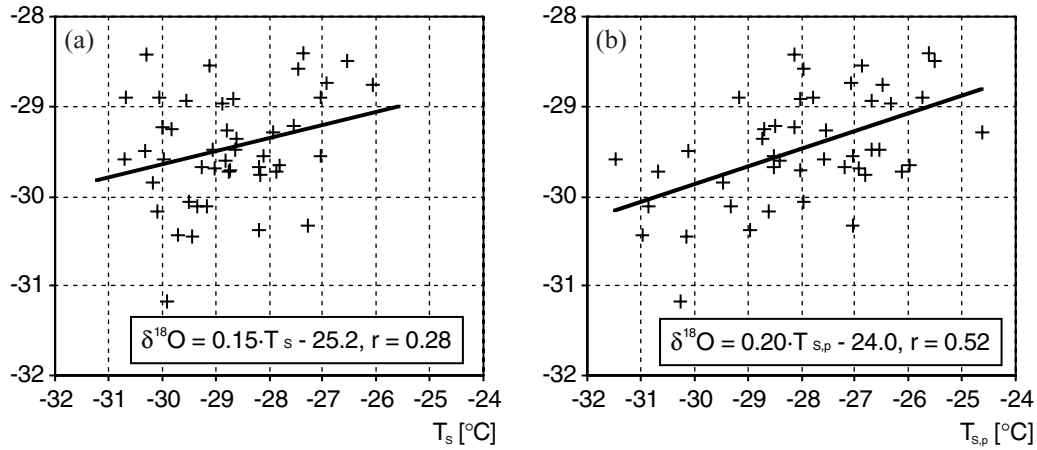

Figure 2. (a) Simulated annual mean $\delta^{18}O$ values versus arithmetic mean surface temperatures T_S in central Greenland for the period 1950–1994. Correlation equation and coefficient of a linear regression (solid line) are given in the text box. (b) Same as Figure 2a but for precipitation-weighted surface temperatures $T_{S,p}$.

Table 1. All Climate Variables Used in Isotope Correlation Analyses for Summit, Central Greenland[a]

Potential Climate Variable Influencing the $\delta^{18}O$ or the *d* Record in Summit, Greenland	Number of Local Regions Significantly Correlated With $\delta^{18}O$ or Excess *d*	Climate Variable Included as Input for Correlation Analysis	Climate Variable Selected for Best Subset
Climate Variables Always Included in Correlation Analysis			
Climate at the precipitation site			
Surface temperature, precipitation-weighted		o / x	
Inversion temperature, precipitation-weighted		o / x	o
Precipitation amount		o / x	
Large-scale pattern indices			
NAO index		o / x	
Seesaw temperature (Oslo-Jakobshavn)		o / x	
Niño-3 index		o / x	
Mean temperature of vapor source regions			
Atlantic SST, 0°–20°N		o / x	
Atlantic SST, 20°–40°N		o / x	x
Atlantic SST, 40°–60°N		o / x	
Atlantic SST, 60°–90°N		o / x	x
Pacific SST, 0°–20°N		o / x	
Pacific SST, 20°–40°N		o / x	
Pacific SST, 40°–60°N		o / x	
Pacific SST, 60°–90°N		o / x	
North America		o / x	
Europe		o / x	
Global Records Used to Identify Additional Local Regions of Significant Correlations			
Surface temperature, precipitation-weighted	1 / –	o	
Inversion temperature, precipitation-weighted	1 / –	o	
Surface temperature, evaporation-weighted	– / –		
Precipitation amount	– / –		
Evaporation amount	– / –		
Sea level pressure	2 / –	o	o
Geopotential height at 500 hPa	2 / –	o	
Relative humidity above surface	1 / –	o	o
Sea ice cover percentage	– / –		

[a] Records used for the $\delta^{18}O$ analysis are marked with "o," and records used for the deuterium excess *d* analysis are marked with "x." Geographical positions of the detected local regions of significant correlation with $\delta^{18}O$ are shown in the correlation maps of Figure 3.

How strong is this link? (4) Are climate phenomena such as ENSO or NAO imprinted in the isotope signal of polar precipitation? If so, which are the most sensitive regions in Greenland and Antarctica?

[6] For Greenland most of our analyses will focus on the central region of this ice sheet, which encloses the Summit region. During the years 1989–1993 several seasons of fieldwork were performed in this region within the framework of the European Greenland Ice Core Project (GRIP) and the U.S. Greenland Ice Sheet Project 2 (GISP2). The observations of numerous glaciological studies enable a detailed comparison of observational data to simulation results for this area of the Greenland ice sheet.

[7] For most parts of Antarctica, annual mean precipitation is <10cm yr^{-1} [*Bromwich*, 1988]. The dryness of this remote area makes observations of interannual $\delta^{18}O$ variations in Antarctica more difficult than in Greenland, since seasonal cycles of $\delta^{18}O$ with wavelengths shorter than 20 cm are obliterated during the firnification process [*Johnsen*, 1977]. Thus, for most Antarctic regions, annual variations of the isotopic composition of precipitation can only be measured for a few years to decades in the uppermost firn layers. Ice cores from coastal regions with much higher precipitation amounts offer the opportunity to study interannual changes of $\delta^{18}O$ in precipitation for longer time periods. One of such drilling sites is the region around Law Dome (66.8°S, 112.8°E) in coastal East Antarctica, where preserved isotopic seasonality has been measured for the last 700 years [*van Ommen and Morgan*, 1997].

2. Methods

2.1. AGCM Description and Boundary Conditions

[8] The applied model was the Hamburg AGCM ECHAM-4 [*Roeckner et al.*, 1996] with both water isotopes $H_2{}^{18}O$ and HDO explicitly cycled through the water cycle of the model [*Hoffmann and Heimann*, 1993]. The simulation was performed in T30 resolution (3.75° by 3.75° spatial grid; 19 vertical levels). Observed monthly values of the global sea ice and sea surface temperature data set (GISST2.2) of the United Kingdom Meteorological Office were prescribed for the period 1950–1994. Atmospheric concentrations of greenhouse gases (CO_2, CH_4, N_2O) but no additional aerosol forcing were also prescribed according to the observations [*Intergovernmental Panel on Climate Change (IPCC)*, 1995].

2.2. Multivariable Linear Regression Analyses

[9] To investigate the possible link between the isotopic composition of precipitation at a specific site in Greenland or Antarctica and other climate variables, e.g., large-scale circulation patterns, a multilinear regression analysis technique is applied at various steps in this study. Since the isotopic composition of a water sample in general represents a precipitation-weighted mean value, we always take precipitation-weighted annual records of $\delta^{18}O$ or deuterium excess *d* as the dependent variable in our regression analyses. As independent input parameters for all the regression analyses, annual records of the following climate variables were chosen: (1) Three annual records were selected for describing the climate at the investigated precipitation site itself - the surface temperature $T_{S,P}$, the temperature of the warmest troposphere model level $T_{I,P}$, further referred to as inversion temperature, and the precipitation amount. For both temperatures, precipitation-weighted records were applied (see also remarks in section 3.1). (2) As general large-scale circulation pattern indices, the simulated NAO index and the Niño-3 index were included in all regression analyses. For the Greenland studies only, we also included the seesaw record of

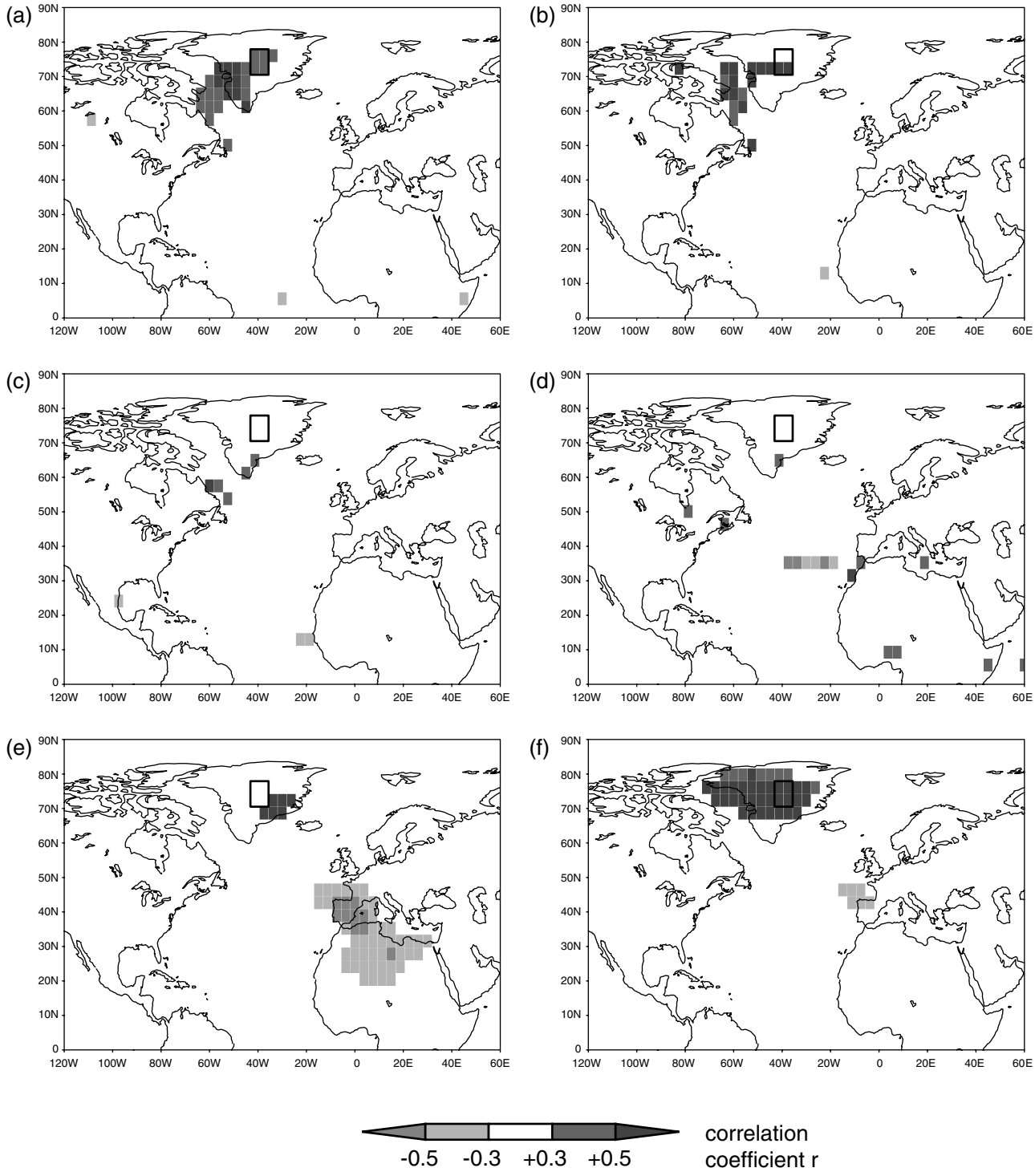

Figure 3. Correlation maps of $\delta^{18}O$ in precipitation in central Greenland (average of outlined rectangle area). (a) Precipitation-weighted surface temperature $T_{S,p}$. (b) Precipitation-weighted inversion temperature $T_{I,p}$. (c) Evaporation-weighted surface temperature $T_{S,e}$. (d) Relative humidity above surface h_S. (e) Sea level pressure. (f) 500 hPa geopotential height Z_{500}. Only areas of significant correlation (probability of chance correlation <5%) are shaded.

surface temperatures from Oslo, Norway, minus Jakobshavn, West Greenland. (3) The most important source areas of water vapor contributing a significant amount to the simulated precipitation of Greenland and Antarctica, respectively, were known from a previous study [*Werner et al.*, 2001]. Since the isotope signature of water vapor in the atmosphere (and thereby also the isotopic signature of precipitation) is related to the temperature during evaporation, we included mean surface temperature records of those source regions in the regression analyses, too.

[10] In a second step we tried to identify additional, more localized strong correlations between the simulated isotope record at the precipitation sites and annual records of nine climate

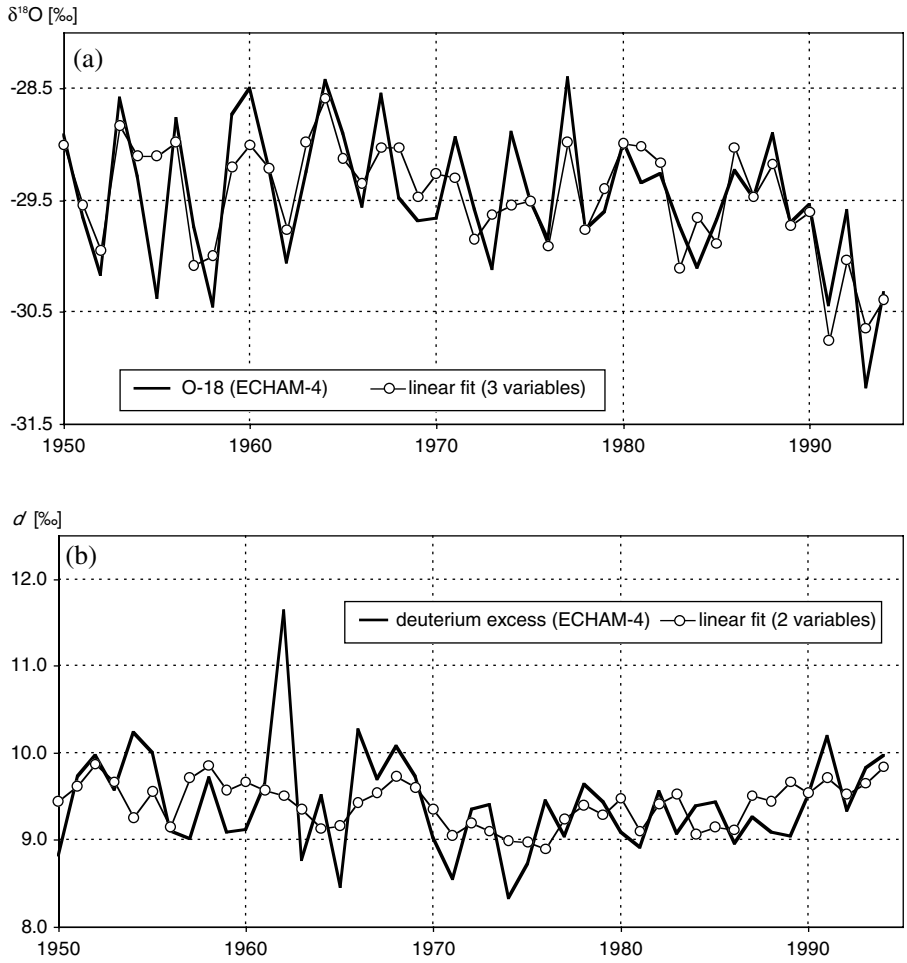

Figure 4. (a) Simulated annual $\delta^{18}O$ record of central Greenland and the fit of a multiple linear regression (three climate variables: inversion temperature west of Greenland, sea level pressure anomalies centered over Spain, and relative humidity of mid-latitudinal Atlantic region) for the period 1950–1994. (b) Simulated annual deuterium excess record of central Greenland and the fit of a multiple linear regression (two climate variables: mean Atlantic SST 20°–40°N and 60°–90°N).

variables. Among those nine climate variables were the precipitation-weighted surface temperatures $T_{S,p}$, evaporation-weighted surface temperatures $T_{S,e}$ (calculated analogous to precipitation-weighted temperatures $T_{S,p}$), precipitation-weighted inversion temperatures $T_{I,p}$, precipitation amount, evaporation amount, sea level pressure (SLP), geopotential height at 500 hPa Z_{500}, relative humidity of the lowest model level above surface h_S, and percentage of sea ice cover. Global correlation maps were used to identify local regions of strong correlation. To reduce the probability of erroneously detecting a climate variable in a local region that is correlated to the isotope signal just by chance, 20 individual correlation maps, each calculated for an arbitrary subset of 36 years of the period 1950–1994, were investigated for each of the nine climate variables. An annual record of any of the nine climate variables in a specific local region was only then chosen to be included in the regression analyses, if a high correlation (probability of chance correlation <5%) was found for at least four coherent grid boxes in all of the 20 individual correlation maps.

[11] In total, between 16 and 23 annual records of different climate variables were included in the various multilinear regression analyses. A best subset regression technique was chosen for determining those climate variables most significantly correlated to the investigated isotope record. Compared to a commonly used step-forward (or step-backward) approach, a best subset technique

Table 2a. Linear Correlation Coefficients (and Explained Variance) of the Simulated Annual $\delta^{18}O$ Signal in Central Greenland and the Three Climate Records of the Best Subset[a]

	Correlation With $\delta^{18}O$ in Central Greenland	
Climate Record	Correlation Coefficient r	Explained Variance, %
$T_{I,p}$ (Greenland, west coast)	0.71	50.4
SLP (Spain)	−0.61	37.8
h_S (midlatitudinal Atlantic)	0.52	27.2

[a] Inversion temperature $T_{I,p}$ at the west coast of Greenland, sea level pressure (SLP) anomalies centered above Spain, and relative humidity h_S of the midlatitudinal Atlantic region.

Table 2b. Cross-Correlation Factors of the Different Climate Records

	Cross Correlation		
Climate Record	$T_{I,p}$	SLP	h_S
$T_{I,p}$ (Greenland, west coast)	1.0	0.35	−0.49
SLP (Spain)		1.0	−0.38
h_S (midlatitudinal Atlantic)			1.0

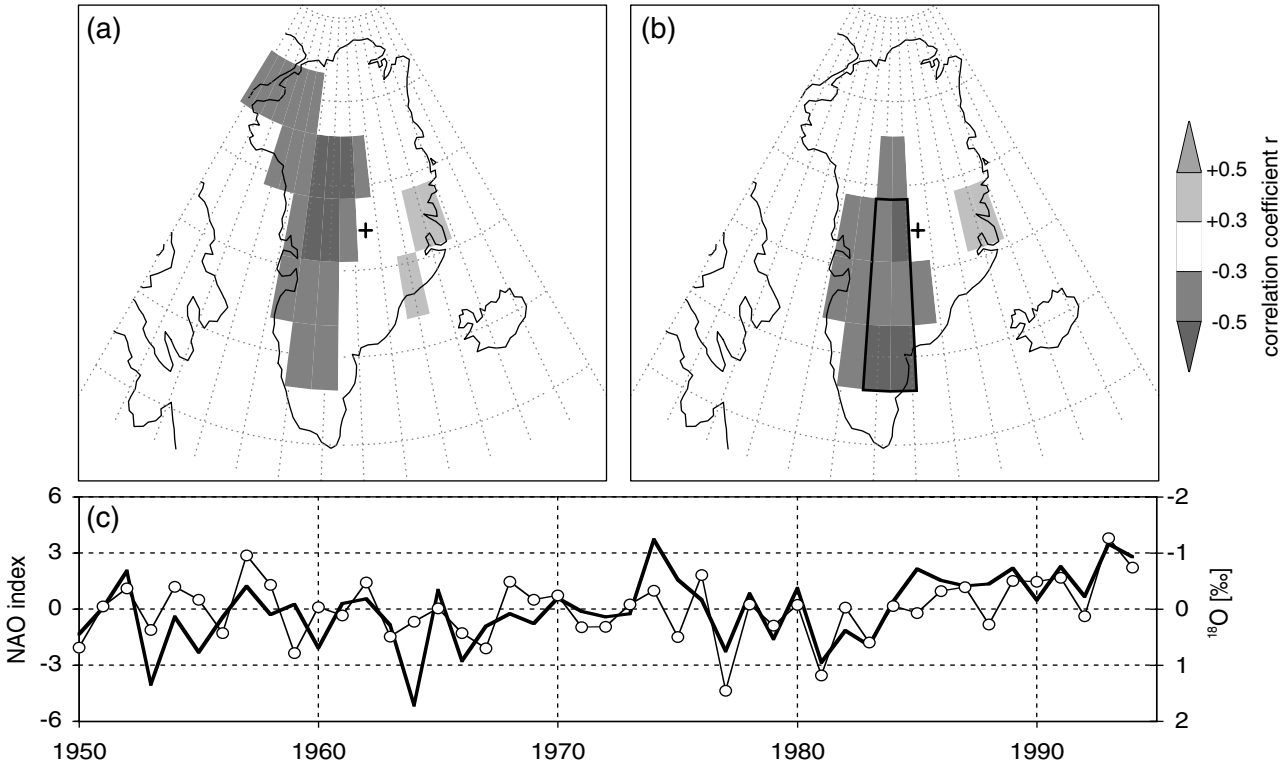

Figure 5. Correlation maps of (a) the simulated annual NAO index and the modeled amount of precipitation in Greenland and (b) the NAO index and the $\delta^{18}O$ values of precipitation. The cross marks the location of the Summit drill site. (c) Time series of the simulated NAO index (black line) and simulated annual $\delta^{18}O$ anomalies (open circles) of the region southwest of Summit (area of the outlined rectangle in Figure 5b). For clarity reasons, the $\delta^{18}O$ axis is reversed.

has the advantage of calculating regression statistics for all possible combination of variable subsets. When selecting the best subset, a balance has to be found between the number of independent variables and the quality of the fit as measured by the residual sum of squares. Obviously, the more variables included the smaller will be the residual sum, but the difference to a regression with fewer variables might be negligible. To balance this, Mallow's Cp statistic was applied for the selection of the best subset. However, even with such a balancing criterion any regression technique that uses a relative high number of independent input variables still contains a risk of erroneously selecting significant statistical correlations, which might have no physical meaning. To reduce such a risk, we applied a "Monte Carlo"-like procedure for the regression analyses. In any investigated case, the best subset of climate variables was not determined for only one regression analysis covering the whole period 1950–1994, but rather best subsets for 20 independent regression analyses, each covering 36 arbitrarily chosen years of the period 1950–1994, were determined. An annual record of any climate variable is only then assumed to have a significant and physical meaningful influence on the investigated isotope signal if it is included in at least half of the 20 best subsets.

3. Results

3.1. Simulated Isotope Record of Summit, Central Greenland

[12] The simulated $\delta^{18}O$ record of the grid box enclosing the Summit region in central Greenland is compared to a combined isotopic record of six individual ice cores of the GRIP and GISP2 drilling sites for the period 1950–1986 [*White et al.*, 1997]. The simulated long-time mean $\delta^{18}O$ value between 1950–1986 ($\delta^{18}O$ = −29.1‰) around Summit is higher than the observations ($\delta^{18}O$ = −35.0‰), which can be explained by the coarse model resolution: The grid box enclosing the Summit region is ∼500 m lower than the true Summit location. The deviation between the mean simulated surface temperature (−27.7°C) and the observations (−32°C) can also be related to the coarse model resolution. The mean simulated deuterium excess value (d = 7.7‰) is in good agreement with recent observations (d = 8.8–9.3‰) of *Hoffmann et al.* [1997] and mean modeled precipitation values (27.1 cm yr^{-1}) are also comparable to observations (23.5 cm yr^{-}). Analyzing the year-to-year variations, the 1σ standard deviation of the modeled $\delta^{18}O$ record ($\Delta\delta^{18}O$ = ±0.66‰) is found to be slightly lower than the observations ($\Delta\delta^{18}O$ = ±0.79‰) for the period 1950–1986 [*White et al.*, 1997]. It is also noticed that the 1σ value of this simulation with prescribed annually varying SST is identical to another ECHAM-4 10-year simulation with a prescribed constant seasonal cycle of SST. This indicates that the year-to-year variability of $\delta^{18}O$ over central Greenland in the model is solely influenced by the simulated internal variability of the atmosphere in higher northern latitudes, and not by the variability of the prescribed SST. Because of the stochastic nature of this internal atmospheric variability it is therefore not possible to model $\delta^{18}O$ anomalies of any specific calendar year in agreement with the observations, as is clearly shown in Figure 1. Nevertheless, an influence of SST variations on the isotope record on longer timescales might still exist and cannot be ruled out by these findings.

3.1.1. Temporal $\delta^{18}O$-temperature-relation. [13] In the previous study of *White et al.* [1997], ∼50% of the variability of the combined GRIP/GISP2 $\delta^{18}O$ record was explained by a multiple linear regression of average coastal Greenland temperature, winter NAO, the annual temperature seesaw between Jakobshavn and Oslo, insolation changes and SST (20°–30°N). However, because

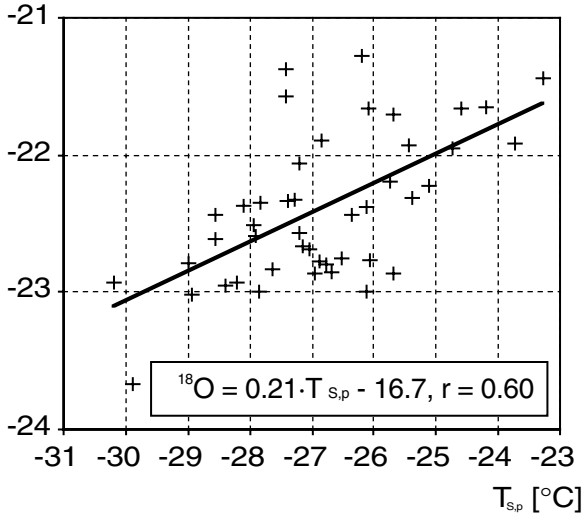

Figure 6. Simulated annual mean $\delta^{18}O$ values versus precipitation-weighted surface temperatures $T_{S,p}$ near Law Dome, Antarctica, for the period 1950–1994. Correlation equation and coefficient of a linear regression (solid line) are given in the text box.

of the lack of temperature observations in the Summit region it remained open, how much of the $\delta^{18}O$ variability reflects the climatic history of a broader region, and how much is related to variability in surface temperatures at the precipitation site. To calculate the latter, we compared the simulated $\delta^{18}O$ record of central Greenland (averaged over four grid boxes in the region 71°–78°N, 36°–43°W) with the surface temperature T_S in the same area for the period 1950–1994 (Figure 2a). The regression between $\delta^{18}O$ and T_S has a slope of m = 0.15‰/°C and a correlation coefficient of r = 0.28, indicating only a weak correspondence between the two time series. To take into consideration that the $\delta^{18}O$ signal is only archived during precipitation events, a record of precipitation-weighted annual surface temperatures $T_{S,p}$

$$T_{S,p} = \sum_i \left(T_{S,I}\mathrm{prec}_i\right) \,/\, \sum_i \left(\mathrm{prec}_i\right) ,$$

with $T_{S,i}$ and prec_i as monthly temperatures (i = 1…12) of an individual year, was also evaluated. This results in a stronger correlation between $\delta^{18}O$ and temperature (r = 0.52, m = 0.20‰/°C), and ~26% of the annual variance of $\delta^{18}O$ can be explained by simultaneous changes of $T_{S,p}$ (Figure 2b).

3.1.2. Other climate parameters influencing the isotope record. [14] It is evident from the preceding analysis that the simulated variability of $\delta^{18}O$ must be influenced by additional climate variables, which are not strongly correlated to surface temperatures on the ice sheet themselves. To identify some of them, a multivariable linear regression analysis between the $\delta^{18}O$ signal in central Greenland and a set of 23 climate records was performed (Table1 and Figure 3). Applying the regression analysis technique described in section 2.2 results in three annual records significantly correlated to the $\delta^{18}O$ signal in central Greenland: the inversion temperatures $T_{I,p}$ at the west coast of Greenland (Figure3b), the sea level pressure above Spain (Figure 3e), and the relative humidity h_S of the narrow midlatitudinal Atlantic region (Figure 3d). All three records together can explain 65% (r = 0.80) of the total variance of the modeled $\delta^{18}O$ record between

Table 3. All Climate Variables Used in Isotope Correlation Analyses for Law Dome, East Antarctica[a]

Potential Climate Variable Influencing $\delta^{18}O$ or the d Record at Law Dome, Antarctica	Number of Local Regions Significantly Correlated With $\delta^{18}O$ or Excess d	Climate Variable Included as Input for Correlation Analysis	Climate Variable Selected for Best Subset
Climate Variables Always Included in Correlation Analysis			
Climate at the precipitation site			
Surface temperature, precipitation-weighted		o / x	o / x
Inversion temperature, precipitation-weighted		o / x	o
Precipitation amount		o / x	
Large-scale pattern indices			
NAO index		o / x	
Niño-3 index		o / x	
Mean temperature of vapor source regions			
Atlantic SST, 0°–20°S		o / x	
Atlantic SST, 20°–40°S		o / x	
Atlantic SST, 40°–60°S		o / x	
Atlantic SST, 60°–90°S		o / x	
Pacific SST, 0°–20°S		o / x	
Pacific SST, 20°–40°S		o / x	
Pacific SST, 40°–60°S		o / x	
Pacific SST, 60°–90°S		o / x	
Indian Ocean SST, 0°–20°S		o / x	o
Indian Ocean SST, 20°–40°S		o / x	
Indian Ocean SST, 40°–60°S		o / x	
Indian Ocean SST, 60°–90°S		o / x	
Global Records Used to Identify Additional Local Regions of Significant Correlations			
Surface temperature, precipitation-weighted	– / –		
Inversion temperature, precipitation-weighted	– / –		
Surface temperature, evaporation-weighted	– / 2	x	x
Precipitation amount	– / –		
Evaporation amount	– / 1	x	
Sea level pressure	– / –		
Geopotential height at 500 hPa	– / 1	x	x
Relative humidity above surface	– / –		
Sea ice cover percentage	– / –		

[a] Records used for the $\delta^{18}O$ analysis are marked with "o," and records used for the deuterium excess d analysis are marked with "x." The geographical positions of the detected local regions of significant correlation with deuterium excess d are shown in the correlation maps of Figure 8.

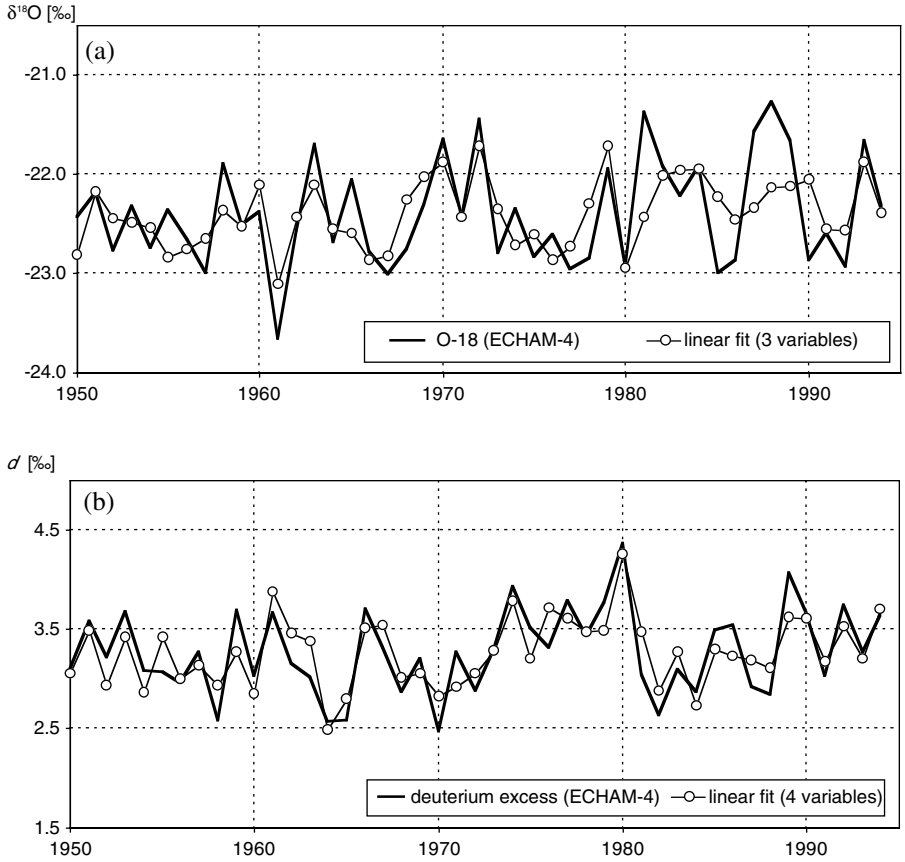

Figure 7. (a) Simulated annual $\delta^{18}O$ record of the region near Law Dome, East Antarctica, and the fit of a multiple linear regression (three climate variables: surface temperature, inversion temperature, and mean Indian Ocean SST 0°–20°S) for the period 1950–1994. (b) Simulated deuterium excess record of the same region, and the fit of a multiple linear regression (four climate variables: surface temperature near Law Dome, evaporation-weighted surface temperature records of two distinct Indian Ocean regions, and 500 hPa geopotential height above southern Atlantic).

1950–1994, and the overall evolution of the $\delta^{18}O$ record is fitted well by a linear combination of these climate variables (Figure 4a). It is somewhat surprising that the inversion temperature $T_{I,p}$ at the west coast of Greenland, and not the temperature directly at the precipitation site in central Greenland, is explicitly included in the regression model. This west coast temperature record $T_{I,p}$ alone accounts for ~50% of the $\delta^{18}O$ variations (Table 2), and one might interpret it as a proxy for the history of air masses transported from the southwest to the Greenland ice sheet. These air masses obviously have a significant impact on the modeled variability of the $\delta^{18}O$ signal in central Greenland. The inversion temperature record $T_{I,p}$ is also related to the other two significant climate records, SLP and h_S, but the cross-correlation factors are rather weak (Table 2).

[15] In contrast to $H_2{}^{18}O$, we could not detect any specific local regions of strong correlation in calculated correlation maps of the deuterium excess anomalies d and the selected climate variables. Thus only 16 records entered in the regression analysis of the deuterium excess (Table 1). The determined best subset consists of only two Atlantic SST records: the mean annual SST record between 60°N and 90°N ($r = -0.26$) and between 20°N and 40°N ($r = 0.35$). The found correlation between the modeled d anomalies and SST changes of the midlatitudinal Atlantic regions is in agreement with previous findings [*Hoffmann et al.*, 1997; *Johnsen et al.*, 1989]. However, both SST records together explain only ~20% ($r = 0.44$) of the total simulated excess variability. As seen in Figure 4b, it is mainly the decadal trend of the deuterium excess record, which is fitted well by these two SST records.

3.1.3. Imprint of the NAO. [16] For a potential reconstruction of a paleo-NAO record by available ice core data, the stated correlation of the sea level pressure and the $\delta^{18}O$ signal in the regression model is of special interest. *Appenzeller et al.* [1998] reported a strongly negative correlation between the NAO record of *Hurrell* [1995] and the annual snow amount derived from the NASA-U core drilled in West Greenland, whereas only a weak correlation was observed for central Greenland. About one third of the total variability could be explained by a linear correlation between the annual NAO record and the net snow accumulation at the NASA-U drill site for the past 130 years. Our model results are in good agreement with the observations of Appenzeller et al. (Figure 5a). Correlation coefficients between the NAO and precipitation amounts are strongly negative west of Summit ($r < -0.5$) and positive at the east coast nearScoresbysund. At the most, about 33% of the interannual variance in modeled precipitation can be related to the NAO. A corresponding correlation of the NAO and the annual mean $\delta^{18}O$ values of precipitation results in a slightly different correlation map (Figure 5b). Positive correlation coefficients are still found at the east coast of Greenland, but the pattern of negative correlation is shifted to the region southwest of the Summit drill site. About 35% of the simulated changes of $\delta^{18}O$ in the latter region can be related to variability in the NAO. Especially, the increasing trend of the simulated NAO index between 1980–1994 is also seen in the $\delta^{18}O$ record. On the contrary, the short-term anomalies of the NAO between 1950–1970 cannot be found in the $\delta^{18}O$ series (Figure 5c). In contrast to $\delta^{18}O$, no significant correlation between the

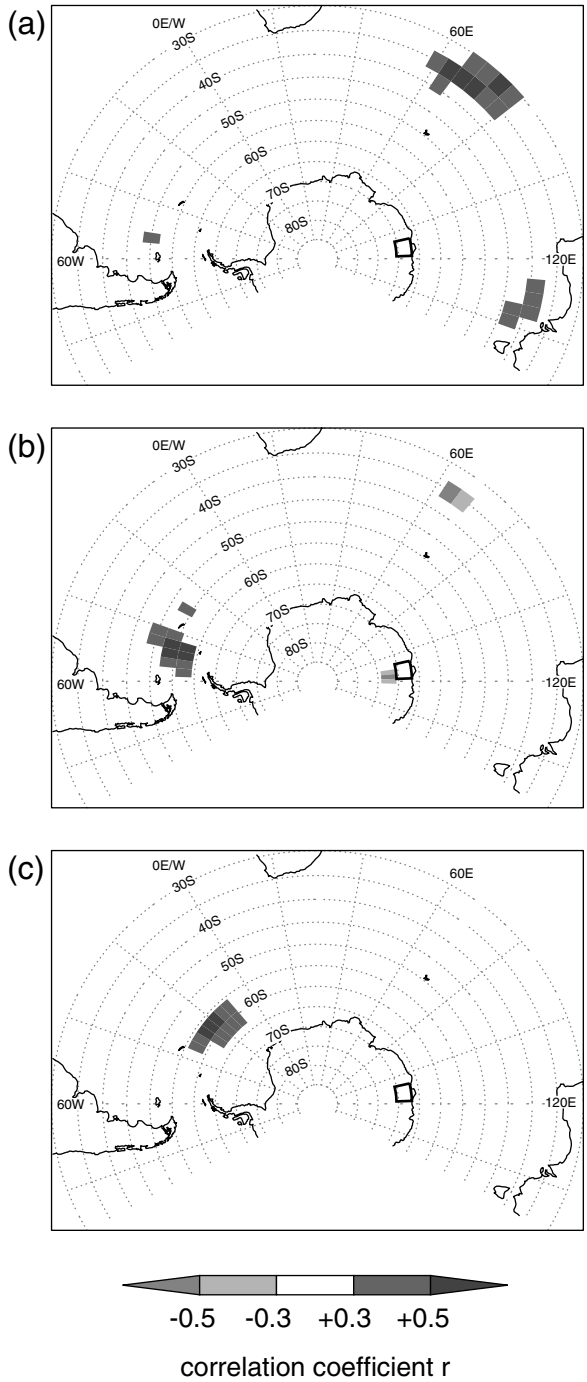

Figure 8. Correlation maps of the deuterium excess d in precipitation near Law Dome, Antarctica (average of outlined rectangle area). (a) Evaporation-weighted surface temperature $T_{S,e}$. (b) Evaporation amount. (c) 500 hPa geopotential height Z_{500}. Only areas of significant correlation (probability of chance correlation <5%) are shaded.

NAO and the deuterium excess values d of precipitation can be found for any Greenland region in this AGCM simulation.

3.2. Simulated Isotope Record of Law Dome, East Antarctica

[17] Mean annual model values of surface temperature (T_S = −26.2°C) and isotopic composition of precipitation ($\delta^{18}O$ = −22.3‰, d = 3.3‰) of the grid box enclosing the Law Dome drilling site are in fair agreement with the observations (T_S = −22°C, $\delta^{18}O$ = −21.7‰ to −22.2‰, d = 3.1 − 4.3‰) for the period 1979–1992 [*Delmotte et al.*, 2000]. The mean simulated seasonal amplitudes of T_S (∼20°C), $\delta^{18}O$ (∼9‰) and d (∼4‰) are also comparable to measurements (16°C, 8‰ and 5‰ [*Delmotte et al.*, 2000]). In contrast to the situation found in central Greenland, the simulated 1σ standard deviation over the period 1950–1994 ($\Delta\delta^{18}O$ = ±0.54‰) differs from another ECHAM-4 simulation with a prescribed constant seasonal SST cycle ($\Delta\delta^{18}O$ = ±0.67‰). This indicates that year-to-year SST variability might have an influence on the isotope record near Law Dome. This region is not only characterized by its coastal location, but also by large gradients in elevation and accumulation rate, which are partly not resolved in the coarse model resolution: The simulated annual precipitation amount of the grid box enclosing Law Dome (33.5 cm yr^{-1}) is lower than the observation at the Law Dome Summit drilling site (64.0 cm yr^{-1}). However, since model values of both temperature and isotopic composition of precipitation are in agreement with the observations, we attribute the disagreement in the precipitation rates to a model deficit of capturing some local coastal precipitation formation rather than to a large-scale erroneous atmospheric circulation in the AGCM simulation.

3.2.1. Temporal $\delta^{18}O$-temperature-relation. [18] A linear correlation of annual values (averages of three coastal grid boxes between 66.8°S and 70.5°S and between 106.9°W and 118.1°W) of surface temperatures T_S and $\delta^{18}O$ values indicates a weak correspondence between both variables (r = 0.34, m = 0.17‰/°C). Using precipitation-weighted annual mean surface temperatures $T_{S,p}$ instead of T_S results in an improved correlation (r = 0.60, m = 0.21‰/°C), shown in Figure 6. The analysis between $\delta^{18}O$ and $T_{S,p}$ reveals that ∼36% of the simulated interannual $\delta^{18}O$ variability around Law Dome can be related to simultaneous changes in surface temperatures.

3.2.2. Other climate parameters influencing the isotope record. [19] Like for the Summit region in Greenland, a multiple linear regression analysis is performed for identifying other climate variables influencing the $\delta^{18}O$ signal near Law Dome. Seventeen climate records were included in this analysis (Table 3), and three climate records were determined to be significantly correlated to the $\delta^{18}O$ record: surface temperatures $T_{S,p}$ at the precipitation site (r = 0.60), inversion temperatures $T_{I,p}$ at the precipitation site (r = 0.58), and mean SST of the Indian Ocean between 0° and 20°S (r = 0.25). For the total period 1950–1994 a linear regression model with these three variables explains 41% of the variability in $\delta^{18}O$ (r = 0.64). A comparison of the time series of the $\delta^{18}O$ record and of the multivariable fit reveals that a linear combination of the three determined climate variables fails to reproduce some strong $\delta^{18}O$ anomalies between 1981 and 1991 (Figure 7a). The cause for these strong simulated $\delta^{18}O$ anomalies remains unclear. A direct correlation with exceptional strong ENSO events (e.g., 1982/1983) is not found. When excluding the period 1981–1991, the correlation between $\delta^{18}O$ and the multivariable fit increases clearly (r = 0.75). For the deuterium excess anomalies d, we included in total 21 climate records in our correlation analysis (Table 3 and Figure 8). The selection of the best subset results in four variables: the surface temperatures $T_{S,p}$ at the precipitation site, the temperature records $T_{S,e}$ of the two regions of the Indian Ocean (Figure 8a), and the Atlantic Z_{500} anomalies northwest of the Antarctic Peninsula (Figure 8c). Together these four variables explain 66% (r = 0.81) of the simulated d anomalies in the Law Dome region between 1950 and 1994 (Figure 7b). None of these four variables appears to dominate in the analysis, and any single record can only explain between 17% and 27% of the d anomalies (Table 4). Additional cross-correlation analysis reveals that only the two $T_{S,e}$ records of the Indian Ocean are partly related to each other.

3.2.3. Imprint of ENSO. [20] A correlation map between the modeled $\delta^{18}O$ record and the Niño-3 index enables the

Table 4a. Linear Correlation Coefficients (and Explained Variance) of the Simulated Annual Deuterium Excess Signal D Near Law Dome, Antarctica, and the Four Climate Records of the Best Subset[a]

	Correlation With d Near Law Dome, Antarctica	
Climate Record	Correlation Coefficient r	Explained Variance, %
$T_{S,p}$ (Law Dome area)	−0.42	17.6
$T_{S,e}$ (Indian Ocean I)	−0.52	27.1
$T_{S,e}$ (Indian Ocean II)	0.48	23.0
Z_{500} (South Atlantic)	0.50	24.7

Table 4b. Cross-Correlation Factors of the Different Climate Records

	Cross Correlation			
Climate Record	$T_{S,p}$	$T_{S,e}$ (I)	$T_{S,e}$ (II)	Z_{500}
$T_{S,p}$ (Law Dome area)	1.0	−0.09	0.04	−0.16
$T_{S,e}$ (Indian Ocean I)		1.0	0.48	0.03
$T_{S,e}$ (Indian Ocean II)			1.0	0.08
Z_{500} (South Atlantic)				1.0

identification of Antarctic regions potentially influenced by ENSO (Figure9a). Significant correlation is found for several coastal regions with highest correlation southeast of the Vostok drill site where 28% of the interannual $\delta^{18}O$ variability can be related to ENSO. However, the dryness of this area (annual precipitation amount <5 cm yr^{-1}) probably inhibits a reconstruction of past ENSO extremes. A better region might be the area southeast of the Law Dome drilling site, where precipitation amounts are much higher. About 21% of the modeled $\delta^{18}O$ variability in this region can be related to the Niño-3 index (r = 0.46). To check the robustness of our model findings, we repeated the analysis for the shorter period 1970–1994, when the prescribed sea ice coverage around Antarctica is more accurate. As is seen in Figure 9b, a similar pattern of positive correlation between $\delta^{18}O$ and the Niño-3 index is simulated for this shorter time period, and to some extent additional regions of negative correlation are found west of the Antarctic Peninsula and in Dronning Maud Land. The latter may be related to coherent variations between ENSO and sea ice coverage around Antarctica, as reported by several authors [e.g., *Gloersen*, 1995]. However, because of the shorter time period the probability of chance correlation has also increased. No significant correlation between the Niño-3 index and the deuterium excess record can be found for any region in Antarctica.

4. Discussion

[21] The various results presented in this study can be discussed with regard to three different aspects: (1) the obvious difference between temporal and spatial $\delta^{18}O$-temperature-relations, (2) the apparently complex relation between the isotope

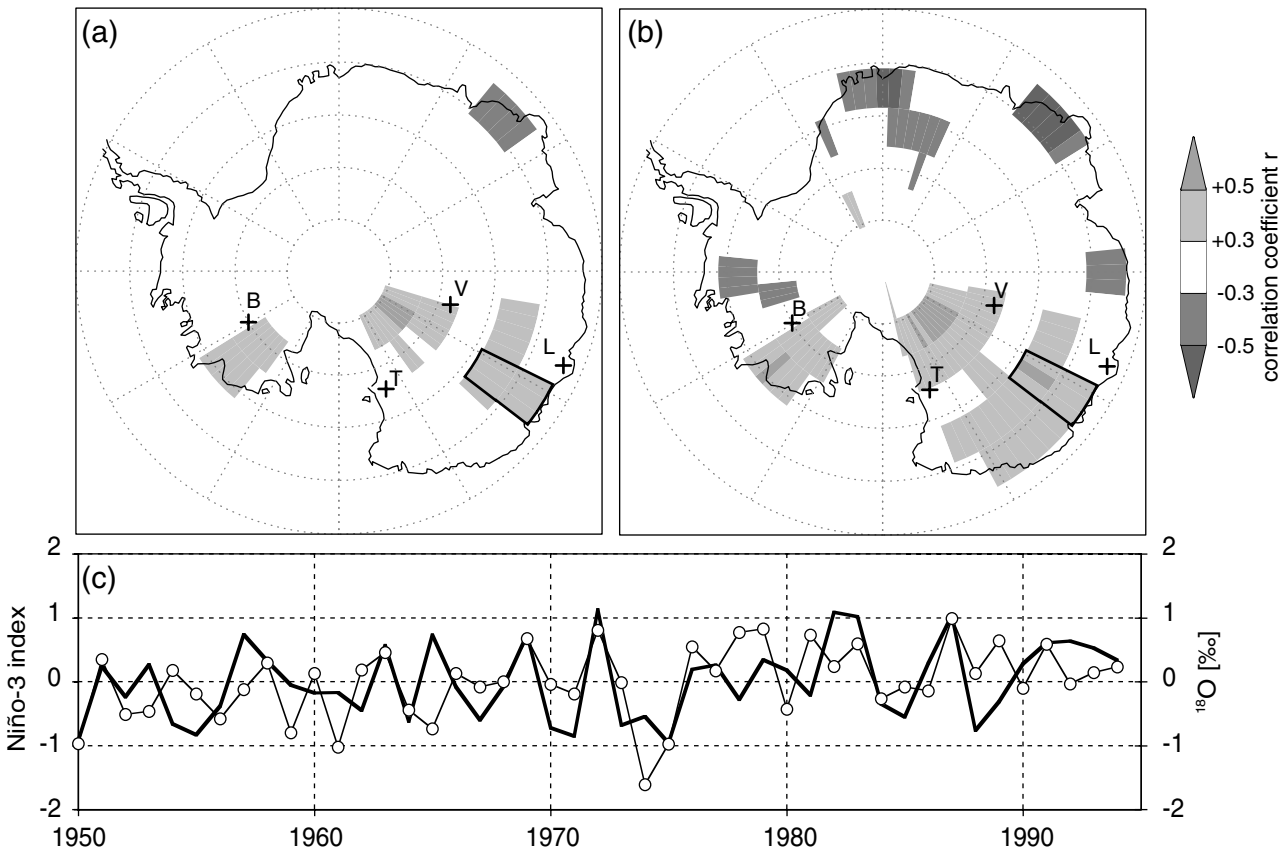

Figure 9. Correlation maps of the Niño-3 index and the modeled $\delta^{18}O$ values of precipitation in Antarctica for (a) the period 1950–1994 and (b) the period 1970–1994. The crosses mark the location of four Antarctic drill sites: V, Vostok; L, Law Dome; T, Taylor Dome; B, Byrd ice core. (c) Time series of the Niño-3 index (black line) and the simulated annual $\delta^{18}O$ anomalies (open circles) of the region southeast of Law Dome (area of the outlined rectangle in Figures 9a and 9b).

records and other influencing climate variables, and (3) the possibility of reconstructing climate indices such as NAO or ENSO from polar ice cores.

4.1. Temporal and Spatial δ^{18}O-Temperature-Relations

[22] For both Greenland and Antarctica the simulated interannual δ^{18}O-*T*-gradient (Summit, $m = 0.15$, $r = 0.28$; Law Dome, $m = 0.17$, $r = 0.34$) is significantly lower that the modeled modern spatial gradient (Greenland, $m = 0.55$, $r = 0.90$; East Antarctica, $m = 0.72$, $r = 0.95$) and also lower than the simulated seasonal gradient (Summit, $m = 0.33$, $r = 0.84$; Law Dome, $m = 0.25$, $r = 0.61$). The simulated rather weak modern temporal δ^{18}O-*T*-gradients agree with the results published by *Cole et al.* [1999]. The δ^{18}O-*T*-relation strengthens if precipitation-weighted temperature records are applied, but the difference between modern temporal and spatial gradients is still obvious. The results of this study extend the recent challenge of the (modern) spatial calibration of the isotope thermometer for glacial-interglacial climate changes [*Jouzel*,1999, and references therein] toward present-day interannual climate variability. Within this context it is also interesting to note that this present-day deviation between temporal and spatial δ^{18}O T_S gradients cannot be explained by the effect of seasonal timing of precipitation, as it is probably valid for glacial-interglacial climate changes on Greenland [*Krinner et al.*, 1997; *Werner et al.*, 2000]. Our findings rather indicate that it may require, in general, different physical mechanisms to explain either large isotope changes between mean states of two very different climate periods (e.g., between the LGM and the present) or relatively small isotope variability during one stable climate period, such as the last century. As already pointed out by *Cole et al.* [1999], year-to-year variability of temperature anomalies can occur as a consequence of changing advection patterns, which simultaneously might change the mixing of air masses with different condensation histories (and thereby different isotopic signatures). According to their study, this variability of the influence of different source regions might be, in general, more significant than the isotope variability forced by temperature changes at the precipitation site itself. On the other hand, long-term glacial-interglacial changes are largely determined by changes in global radiation and other forcing. The effect of year-to-year variability in the advection patterns is probably negligible, especially if only the mean state of glacial versus interglacial climate is compared. A general change of the influence of different vapor source regions during the different climate stages could of course occur, too. But this does not seem to play an important role for Greenland or Antarctica if LGM and present-day climate simulations are compared [*Werner et al.*, 2001].

4.2. Interpretation of Interannual Isotope Variability

[23] The results of the various multilinear regression analyses reveal that the simulated temporal isotope variability is influenced not only by temperature, but also by several other climate variables. It also seems to be evident that isotope records at different locations are not always influenced by the same set of climate variables. For central Greenland the δ^{18}O variability is strongly related to inversion temperatures at the west coast of Greenland and above the Davis Strait. Variability in the long-range transport of Atlantic air masses, which can be characterized by both humidity values around 30°–40°N and sea level pressure anomalies centered over Spain, is also a significant factor for changing the δ^{18}O signal in central Greenland. These results are in broad agreement with the study of *White et al.* [1997], where average coastal Greenland temperatures, NAO, and SST between 20° and 30°N were identified as significantly influencing a stacked GRIP/GISP2 δ^{18}O record. But our simulation findings indicate that it is mainly the temperature at the west coast of Greenland, the low-latitude part of the NAO and rather relative humidity changes than SST anomalies of the subtropical Atlantic, which are influencing the δ^{18}O signal. Regarding the simulated deuterium excess *d* anomalies, interannual to decadal variability appears to be an even more complex signal. Decadal trends seem to be caused by SST changes in the midlatitudinal and northern Atlantic. However, the simulated year-to-year variability of the deuterium excess could not be related to simultaneous changes of investigated climate variables, neither at the precipitation site nor at potential evaporation regions. Thus those year-to-year deuterium excess changes are maybe even more related to internal atmospheric mixing processes of water masses from different evaporation sites rather than to temperature or humidity changes at one specific site, only.

[24] In contrast to Greenland, the variability of isotopic anomalies in precipitation near Law Dome in Antarctica seems to follow a more "classical" interpretation of isotope records. While the δ^{18}O anomalies were found to be mainly related to temperatures during precipitation formation at the precipitation site itself, the strength of the *d* excess anomalies depends on evaporation temperatures plus a second temperature-dependent kinetic effect occurring during the formation of precipitation at very low temperatures [*Jouzel and Merlivat*, 1984]. Evaporation temperature changes at two distinct regions of the southern Indian Ocean have been identified as significantly affecting the deuterium excess signal *d* in the investigated region around Law Dome.

[25] Similar to the findings of *Cole et al.* [1999] we find only a weak correlation ($r = 0.13$) between δ^{18}O and precipitation amount anomalies near Summit, Greenland, but a much stronger correlation ($r = 0.40$) near Law Dome, Antarctica. Also in agreement with their results is the rather weak δ^{18}O-temperature-relation ($r = 0.34$) at the Law Dome region, if arithmetic mean temperatures are investigated. However, if we apply precipitation-weighted temperature anomalies, the δ^{18}O-temperature-relation significantly improves ($r = 0.60$) and is stronger than the δ^{18}O-precipitation-relation. Cole et al. also mention in their article that precipitation amounts are strongly correlated to temperature, which could explain the positive δ^{18}O-precipitation-correlation over Antarctica seen in their study. Unfortunately, they did not distinguish between arithmetic mean and precipitation-weighted mean temperature records. This prevents a further comparison of the direct effect of precipitation amount anomalies on simulated δ^{18}O changes between both GCM studies.

[26] In general, we conclude that it is possible to decipher large parts of the interannual variability of isotope records from both Greenland and Antarctica by multilinear regression analyses. Whether one chooses a stepwise regression technique [e.g., *White et al.*, 1997], or a best subset regression technique, such as in this study, does not seem to strongly influence the results. Far more important is the selection and the completeness of the climate records prescribed as independent input variables. One should also mention that a simple regression analysis, which includes all possible candidates influencing the isotope records but does not attempt to select a "best" subset, might give some misleading results. For example, a simple regression analysis of the modeled δ^{18}O signal near Summit and all 23 climate variables listed in Table 1 results in a very good fit of the isotope signal ($r = 0.90$). However, only the three variables of the found best subset are, in fact, needed for a similar good correlation ($r = 0.80$). Further tests showed that if we prescribed 23 records of pure "white noise" instead of physical meaningful climate records as input parameters, we would also achieve a good fit of the isotope record ($r \approx 0.75$). On the contrary, a simple regression analysis with only three white noise records shows a much weaker correlation with the δ^{18}O signal ($r \approx 0.26$)

4.3. Paleoreconstruction of NAO and ENSO

[27] For a possible reconstruction of past climate indices, such as NAO or ENSO, from polar ice cores, only the δ^{18}O records appear to be useful, since no correlation was found between the

deuterium excess *d* and NAO or ENSO, neither in Greenland nor in Antarctica. These findings seem to stand in some contradiction to the reported correlation between the deuterium excess *d* in the Law Dome region and SST anomalies of two distinct regions of the Indian Ocean. One might argue that if the *d* anomalies are related to Indian Ocean SST anomalies, there should also be also a correlation between deuterium excess *d* and the ENSO signal, which is known to influence Indian Ocean SST with a time lag of several months. Indeed, correlation analyses of our prescribed SST data set show a time-lagged correlation ($r = 0.28$) between the Niño-3 index and the arithmetic mean SST record of the Indian Ocean region shown in Figure 8. However, this correlation significantly decreases to its half when we apply an evaporation-weighted SST record of this region. On the contrary, the deuterium excess signal is more strongly related to the evaporation-weighted SST record than to the arithmetic mean SST record. This finding seems to be reasonable since the deuterium excess signal is controlled by changes of both temperature and relative humidity during the evaporation process [*Johnsen et al.*, 1989; *Merlivat and Jouzel*, 1979]. Consequently, direct correlation between the deuterium excess *d* and the Niño-3 index remains low, even if we assume various time lags between 1 and 18 months for the deuterium excess signal in our analyses.

[28] For the $\delta^{18}O$ records, our results indicate that decadal variations of the NAO might be identified by $\delta^{18}O$ anomalies in western Greenland ice cores, while shorter year-to-year NAO variations are masked by other atmospheric variability. For Antarctica, our results raise the serious question if a reconstruction of paleo-ENSO events from $\delta^{18}O$ anomalies in Antarctic ice cores will be successful. The correlation found in our simulation is rather weak and did not increase significantly, even if we assume a possible time-lagged response of the $\delta^{18}O$ signal between 1 and 18 months. With a maximum of 20% interannual $\delta^{18}O$ variability explained by the Niño-3 index, investigations in paleo-$\delta^{18}O$ archives closer located to the central ENSO region (e.g., tropical ice cores) seem more appropriate. However, for both Greenland and Antarctica it should not be forgotten that the findings presented here are purely based on one single ECHAM-4 GCM model simulation. Any general model deficits with regard to NAO- or ENSO-related interannual atmospheric variability (e.g., as discussed by *Latif et al.* [2000]) might hide some stronger correlation occurring in reality. In order to confirm those model results, larger ensembles of isotope AGCM simulations with different GCM models should therefore be conducted. However, to our knowledge, so far no other isotope GCM simulation over a comparable time period and with comparable prescribed boundary conditions has been performed and published.

5. Conclusions

[29] This ECHAM-4 simulation shows clearly the general usefulness of isotope AGCM modeling for studying interannual to decadal isotope variability. For two drilling sites in Greenland and Antarctica, the simulated mean isotopic signature of precipitation and the strength of interannual variability, respectively, are in fair agreement with the observations for the period 1950–1994. The results indicate that about one third of the $\delta^{18}O$ variability can be related to simultaneous surface temperature anomalies at the precipitation sites and that the temporal isotope-temperature-relation between 1950–1994 is significantly weaker than the modeled spatial relation, in both Greenland and Antarctica. Multivariable linear regression analyses reveal that especially the isotopic signature of precipitation near Summit, Greenland, seems to be a highly complex signal integrating interannual changes of various climate variables. Further correlation analyses show that the strength of past decadal NAO changes might be constructed from $\delta^{18}O$ anomalies found in western Greenland ice cores, while a reconstruction of past ENSO events from Antarctic $\delta^{18}O$ records seems doubtful.

[30] Although this article focuses on the polar regions, the presented AGCM simulation was performed on a global scale. Thus the described regression analysis technique could be applied for any region of interest to enhance our understanding of observed isotope variability on interannual to decadal timescales. Another aspect of future research might be the identification of potential regions best suited for a reconstruction of past ENSO events by the various water isotope archives.

[31] **Acknowledgments.** We gratefully thank Mojib Latif, Georg Hoffmann, and two anonymous reviewers for their helpful comments on this manuscript. Parts of this study were supported by the European Community (ENV4-CT95-0130). Computing facilities were kindly provided by the German Climate Computing Center (DKRZ) in Hamburg.

References

Appenzeller, C., T. F. Stocker, and M. Anklin, North Atlantic Oscillation dynamics recorded in Greenland ice cores, *Science*, *282*, 446–449, 1998.

Bromwich, D. H., Snowfall in high southern latitudes, *Rev. Geophys.*, *26*, 149–168, 1988.

Bromwich, D. H., A. N. Rogers, P. Kallberg, R. I. Cullather, J. W. C. White, and K.J. Kreutz, ECMWF analyses and reanalyses depiction of ENSO signal in Antarctic precipitation, *J. Clim.*, *13*(8), 1406–1420, 2000.

Charles, C. D., D. H. Rind, J. Jouzel, R. D. Koster, and R. G. Fairbanks, Glacial-interglacial changes in moisture sources for Greenland: Influences on the ice core record of climate, *Science*, *263*, 508–511, 1994.

Cole, J. E., D. Rind, R. S. Webb, J. Jouzel, and R. Healy, Climatic controls on interannual variability of precipitation $\delta^{18}O$: Simulated influence of temperature, precipitation amount, and vapor source region, *J. Geophys. Res.*, *104*, 14,223–14,235, 1999.

Dansgaard, W., Stable isotopes in precipitation, *Tellus*, *16*, 436–468, 1964.

Delmotte, M., V. Masson, J. Jouzel, and V. I. Morgan, A seasonal deuterium excess signal at Law Dome, coastal eastern Antarctica: A southern ocean signature, *J. Geophys. Res.*, *105*, 7187–7197, 2000.

Gloersen, P., Modulation of hemispheric sea-ice cover by ENSO events, *Nature*, *373*, 503–506, 1995.

Hoffmann, G., and M. Heimann, Water tracers in the ECHAM General Circulation Model, in *Isotope Techniques in the Study of Past and Current Environmental Changes in the Hydrosphere and the Atmosphere: Proceedings of an International Symposium on Applications of Isotope Techniques in Studying Past and Current Environmental Changes in the Hydrosphere and the Atmosphere*, Int. At. Energy Agency, Vienna, 1993.

Hoffmann, G., M. Stievenard, J. Jouzel, J. W. C. White, and S.J. Johnsen, Deuterium excess record from central Greenland (modelling and observations), in *International Symposium on Isotope Techniques in the Study of Past and Current Environmental Changes in the Hydrosphere and the Atmosphere*, edited by P. Murphy, pp. 591–602, Int. At. Energy Agency, Vienna, 1997.

Hoffmann, G., M. Werner, and M. Heimann, Water isotope module of the ECHAM atmospheric general circulation model: A study on time scales from days to several years, *J. Geophys. Res.*, *103*, 16,871–16,896, 1998.

Hurrell, J.W., Decadal trends in the North Atlantic Oscillation-Regional temperatures and precipitation, *Science*, *269*, 676–679, 1995.

Intergovernmental Panel on Climate Change (IPCC), Climate change 1995, in *The Supplementary Report to the IPCC Scientific Assessment*, edited by T. Houghton, B. A. Callander and K. V. Varney, 200 pp., Cambridge Univ. Press, New York, 1995.

Johnsen, S. J., Stable isotope homogenization of polar firn and ice, in *Symposium on Isotopes and Impurities in Snow and Ice*, *IAHS AISH Publ.*, *118*, 210–219, 1977.

Johnsen, S. J., W. Dansgaard, and J. W.C. White, The origin of Arctic precipitation under present and glacial conditions, *Tellus, Ser. B*, *41*, 452–468, 1989.

Joussaume, J., R. Sadourny, and J. Jouzel, A general circulation model of water isotope cycles in the atmosphere, *Nature*, *311*, 24–29, 1984.

Jouzel, J., Calibrating the isotopic paleothermometer, *Science*, *286*, 910–911, 1999.

Jouzel, J., and L. Merlivat, Deuterium and δO in precipitation: Modeling of the isotopic effects during snow formation, *J. Geophys. Res.*, *89*, 11,749–11,757, 1984.

Jouzel, J., G. L. Russell, R. J. Suozzo, R. D. Koster, J. W. C. White, and W. S. Broecker, Simulations of the HDO and $H_2{}^{18}O$ atmospheric cycles using the NASA GISS General Circulation Model: The seasonal cycle for present-day conditions, *J. Geophys. Res.*, *92*, 14,739–14,760, 1987.

Krinner, G., C. Genthon, and J. Jouzel, GCM analysis of local influences on ice core δ signals, *Geophys. Res. Lett.*, *24*, 2825–2828, 1997.

Latif, M., K. Arpe, and E. Roeckner, Oceanic control of decadal North Atlantic sea level pressure variability in winter, *Geophys. Res. Lett.*, *27*, 727–730, 2000.

Merlivat, L., and J. Jouzel, Global climatic interpretation of the deuterium-^{18}O relationship for precipitation, *J. Geophys. Res.*, *84*, 5029–5033, 1979.

Roeckner, E., K. Arpe, L. Bengtsson, M. Christoph, M. Claussen, L. Dümenil, M. Esch, M. Giorgetta, U. Schlese, and U. Schulzweida, The atmospheric General Circulation Model Echam-4: Model description and simulation of present-day climate, Max-Planck-Inst. for Meteorol., Hamburg, Germany, 1996.

Shuman, C. A., R. B. Alley, S. Anandakrishnan, J. W. C. White, P. M. Grootes, and C. R. Stearns, Temperature and accumulation at the Greenland Summit: Comparison of high-resolution isotope profiles and satellite passive microwave brightness temperature trends, *J. Geophys. Res.*, *100*, 9165–9177, 1995.

van Ommen, T. D., and V. I. Morgan, Peroxide concentrations in the Dome Summit South ice core, Law Dome, Antarctica, *J. Geophys. Res.*, *101*, 15,147–15,152, 1996.

van Ommen, T. D., and V. I. Morgan, Calibrating the ice core paleothermometer using seasonality, *J. Geophys. Res.*, *102*, 9351–9357, 1997.

Vimeux, F., V. Masson, J. Jouzel, M. Stievenard, and J. R. Petit, Glacial-interglacial changes in ocean surface conditions in the Southern Hemisphere, *Nature*, *398*, 410–413, 1999.

Werner, M., U. Mikolajewicz, M. Heimann, and G. Hoffmann, Borehole versus isotope temperatures on Greenland: Seasonality does matter, *Geophys. Res. Lett.*, *27*, 723–726, 2000.

Werner, M., M. Heimann, and G. Hoffmann, Isotopic composition and origin of polar precipitation in present and glacial climate simulations, *Tellus, Ser. B*, *53*, 53–71, 2001.

White, J. W. C., L. K. Barlow, D. Fisher, P. Grootes, J. Jouzel, S. J. Johnsen, M. Stuiver, and H. Clausen, The climate signal in the stable isotopes of snow from Summit, Greenland: Results of comparisons with modern climate observations, *J. Geophys. Res.*, *102*, 26,425–26,439, 1997.

M. Heimann and M. Werner (corresponding author), Max-Planck-Institute for Biogeochemistry, P.O. Box 10 01 64, Carl-Zeiss Promenade 10, D-07701 Jena, Germany. (martin.heimann@bgc-jena.mpg.de; martin.werner@bgc-jena.mpg.de)